

# F 44

## NORMAL ZEEMAN EFFECT

Christina Schwarz

Martin-I. Trappe

(Dated: February 28, 2006)

### Abstract

We first investigate the normal Zeeman Effect of the red Cd line emerging from a gas discharge lamp in the presence of an external magnetic field. Especially, we analyse the line splitting of the transverse as well as the longitudinal Zeeman Effect utilizing a Lummer-Gehrcke plate and in the course of that we consider the polarisation states of the occurring lines. Due to the experimental realization we obtain Bohr's Magneton  $\mu_B$  and the specific electron charge  $e$ . As a second task we determine two wavelengths of a Cd-Hg-lamp in the red range using a CCD spectrometer and the visible Ne lines for calibration.

### Introduction

The Zeeman Effect denotes the splitting of atomic energy levels due to the action of an external magnetic field. The effect was first predicted by H. A. Lorentz in 1895 as part of his classical theory of the electron and experimentally confirmed a few years later by P. Zeeman who found a line triplet instead of a single spectral line observing orthogonal to a magnetic field as well as a line doublet parallel to the magnetic field.

This work is based on [1].

### Experimental setup, measurements and results

**Spectroscopy of the Zeeman Effect** The observation of the normal Zeeman Effect is only possible for transitions between atomic states with total spin  $S = 0$ . In our case we consider the transition  $^1D_2 (J = 2, S = 0) \rightarrow ^1P_1 (J = 1, S = 0)$  of Cd. Without an external magnetic field the wavelength corresponding to this transition is  $\lambda_0 = 644\text{nm}$  (see Figure 1).

For the angular-momentum component in the direction of the magnetic field holds

$$J_z = M_J \cdot \hbar \quad (1)$$

$$\text{with } M_J = J, J - 1, \dots, -J + 1, -J \quad (2)$$

Therefore, the term with the angular momentum  $J$  is split into  $2J + 1$  equidistant Zeeman components distinguished by the value of  $M_J$ . The energy interval of the adjacent components  $M_J, M_{J+1}$  is

$$\Delta E = \mu_B \cdot B \quad (3)$$

To determine the magnetic field strength one has in principle to measure the hysteresis of the used electromagnet. Our results are represented in Figure 2 but since our measuring

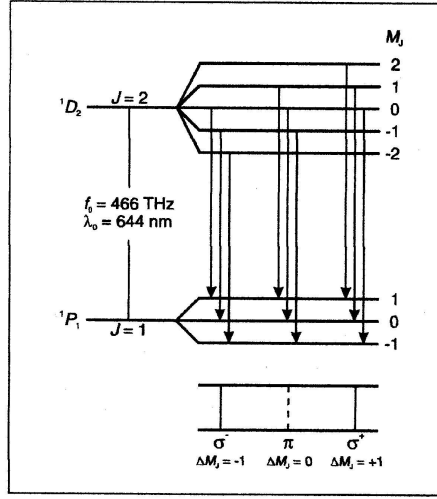


Figure 1: Schematic diagram of the transition  $^1D_2$  ( $J = 2$ ,  $S = 0$ )  $\rightarrow$   $^1P_1$  ( $J = 1$ ,  $S = 0$ ) of cadmium

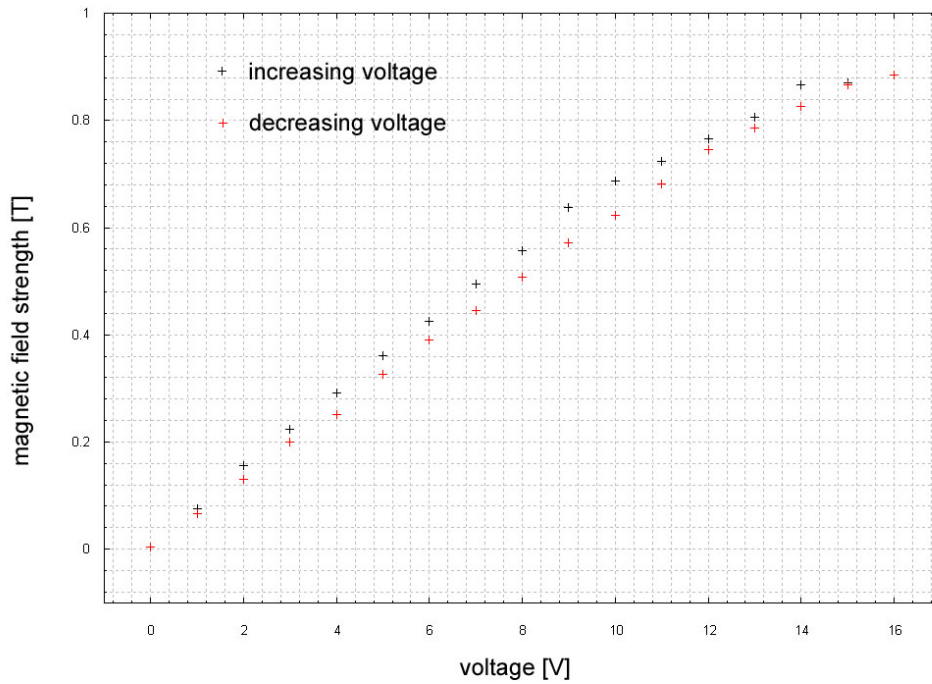


Figure 2: Magnetic field strength  $B$  as a function of applied voltage measured with a hall generator.

devices were not very precise we take the reference values of our electromagnet (see Table I). For a transition with  $\Delta M_J = 0$  no photons propagate in the direction of the magnetic field. Thus the  $\pi$ -component cannot be observed parallel to the magnetic field in opposite to the transversal direction. The complete measuring apparatus together with the latter configuration is illustrated in Figure 3. Here the crucial device is a Lummer-Gehrcke plate (see Figure 4) that splits a beam with angle of incidence  $\beta$  several times while the splitted beams interfere and pass through a lense which is focussed to infinity. With a telescope (see Figure 3) we can observe the occuring interference pattern if the interference condition  $\Delta = 2d\sqrt{n^2 - \sin^2 \alpha_k} = k\lambda$  is fulfilled (see Figure 4). The pattern consists of many parallel stripes representing the different orders of interference. The telescope can be adjusted to read off the distances between those stripes. First we take into account the case of transverse configuration, i.e. the direction of observation is perpendicular to the direction of the magnetic field.

For the magnetic field strength  $B = 0$  we only observed the distances  $\Delta a$  between the different

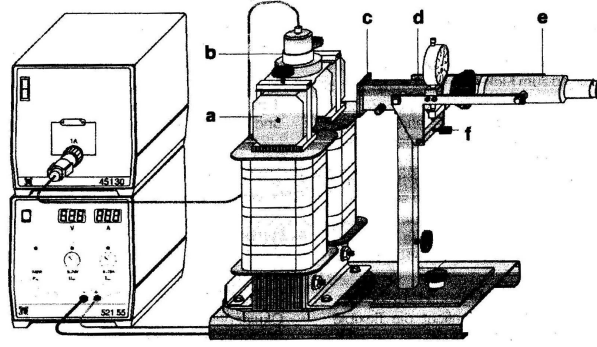


Figure 3: Schematic diagram of the whole measuring apparatus for the determination of the Zeeman Effect. a) magnetic pole pieces b) Hg-Cd lamp c) red filter, polarization filter, quarter-wavelength foil d) Lummer-Gehrcke plate e) telescope with ocular f) height adjustment for telescope

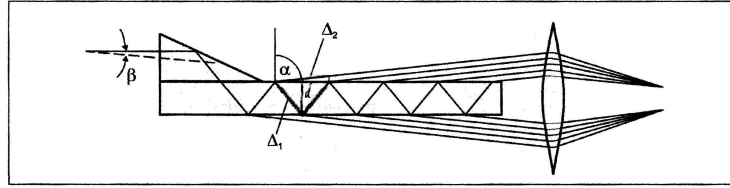


Figure 4: Schematic diagram of the Lummer-Gehrcke plate. Here a light ray with an angle  $\beta$  of incidence is split into different rays with an optical path difference of  $\Delta = n \Delta_1 - \Delta_2$  between two adjacent emerging rays.

orders of interference (see Figure 5) while for  $B > 0$  we could observe the split up of the lines according to the Zeeman Effect (see Figure 5a). The distance between the lines of the emerging triplet is denoted as  $\delta a$ . Analogously, we considered the longitudinal configuration (see Figure 6). Here the interference pattern is altered with respect to the case of transverse configuration. The  $\pi$ -component of the triplet vanishes since the probability of photons propagating parallel to the magnetic field is zero. Using polarization filters and quarter-wavelength plates one can draw conclusions on the polarization states of the emitted photons. Increasing the magnetic

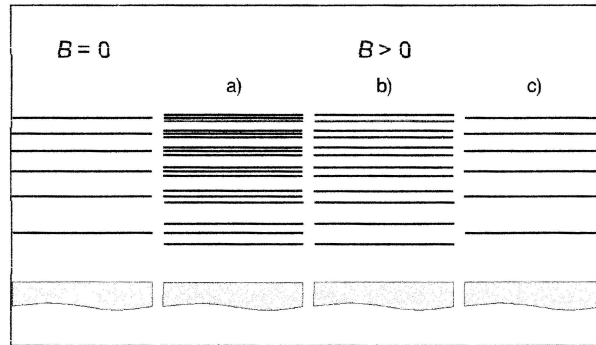


Figure 5: Illustration of the interference pattern of the Zeeman Effect observed in the transverse configuration a) without polarization filter b) with polarization direction of the filter perpendicular to the magnetic field c) with polarization direction of the filter parallel to the magnetic field

field strength from 0.688 T to 0.885 T we obtain both  $\delta a$  and  $\Delta\lambda$  as a function of  $B$  using

$$\Delta\lambda = \frac{\delta a}{\Delta a} \cdot \frac{\lambda^2}{2d\sqrt{n^2 - 1}} \quad (4)$$

With equation (3) the result for Bohr's magneton is  $\mu_B = 8.6(7) \cdot 10^{-24} \frac{\text{J}}{\text{T}}$ . The error estimate emerges from the following consideration. As seen in Table IV we derived  $\Delta\lambda$  depending on the

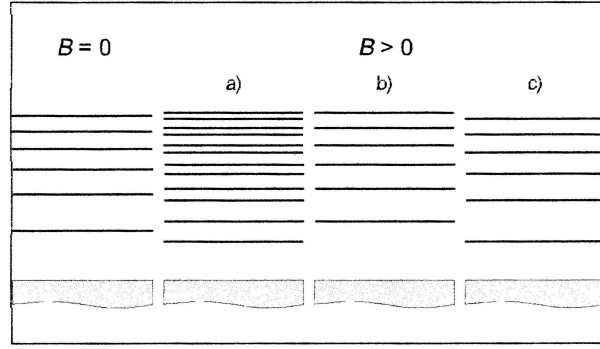


Figure 6: Illustration of the interference pattern of the Zeeman Effect observed in the longitudinal configuration a) without both polarization filter and quarter-wavelength foil b),c) with polarization filter and quarter-wavelength foil to demonstrate counterclockwise and clockwise-circular polarization

magnetic field strength. Every value of  $B$  leads to 28 values of  $\Delta\lambda$  that give the mean value  $\overline{\Delta\lambda}$  of  $\Delta\lambda$  (see Table V). As the error  $\Delta(\overline{\Delta\lambda})$  we take the root mean square deviation of  $\overline{\Delta\lambda}$ . Then  $\Delta E$  follows from  $\overline{\Delta\lambda}$ . Together with the four magnetic field strengths equation (3) yields four values  $\mu_B$  (see Table V). The mean value of  $\mu_B$  gives our result with the root mean square deviation as error.

This value coincides with the bibliographical reference  $\mu_{B,\text{lit}} = 9.274 \cdot 10^{-24} \frac{\text{J}}{\text{T}}$ . From  $\mu_B$  the specific electron charge  $e = \frac{2m_e\mu_B}{\hbar} = 1.48(12) \cdot 10^{-19} \text{C}$  follows immediately which coincides with the value from literature  $e = 1.60 \cdot 10^{-19} \text{C}$  as well.

**Determination of a Cd line** In this section we describe the determination of the wavelength of two lines in the red range using the CCD-spectrometer illustrated in Figure 7. The first task is the calibration of the spectrometer that is performed via the spectrum of a

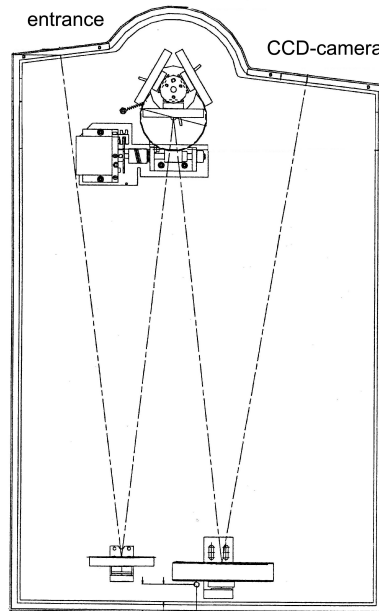


Figure 7: Schematic diagram of the TRIAX 550 spectrometer. The optical path is drawn. In the upper part the adjustable grating that decomposes light in its spectrum is illustrated.

neon lamp. The references of the considered range of the neon spectrum are taken from [2]. We measured the visible range of cadmium as well as neon (see Figure 8) and performed a gaussian fit for every emerging peak (see Figure 9 as an example). So we were able to read off

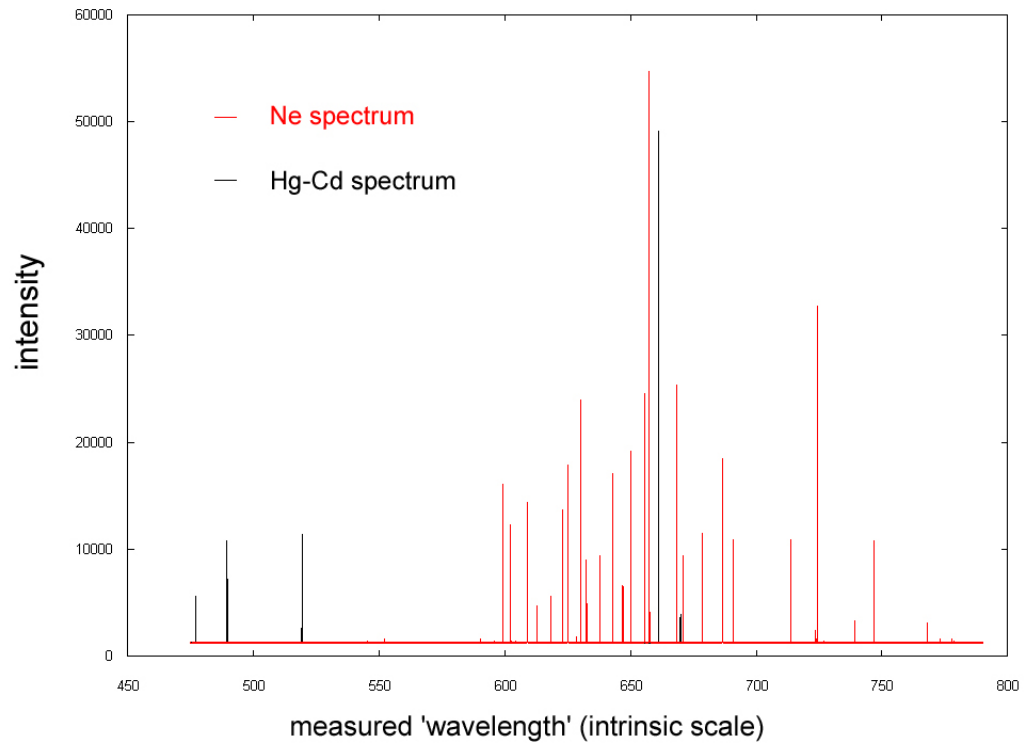


Figure 8: Representation of the measured visible spectrum of the used neon lamp and Hg-Cd lamp respectively.

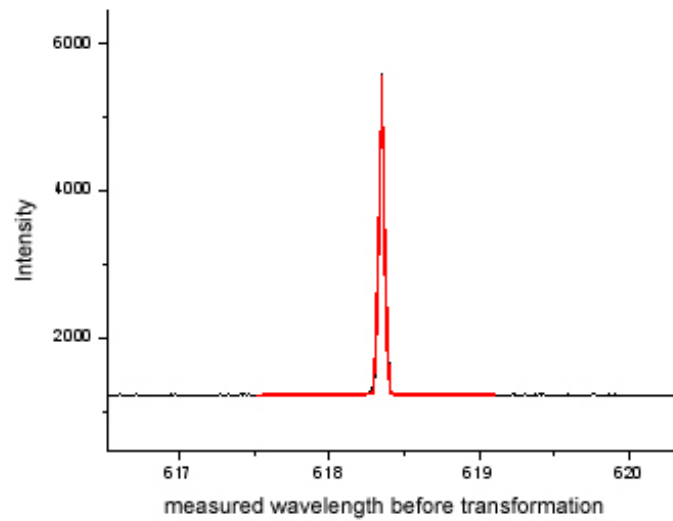


Figure 9: Here the black line represents the intensity of the spectrum as a function of the measured wavelengths while the red line is the gaussian fit of a spectral peak.

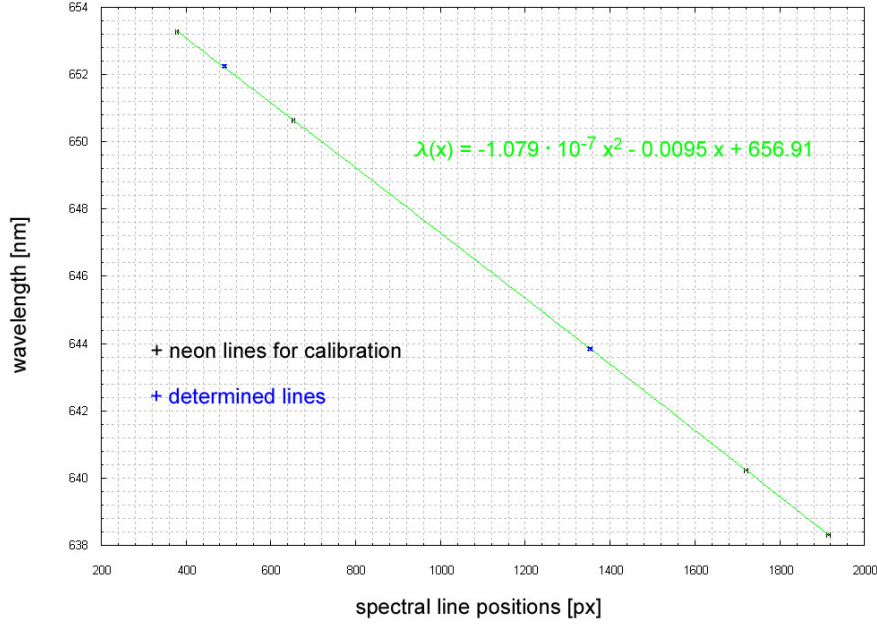


Figure 10: Calibration between line positions determined by the spectrometer and the reference spectrum taken from neon.

the position and the FWHM of every peak according to the pixel scale of the spectrometer. With the reference data we could finally derive a transformation between the measured scaled wavelengths and the wavelengths in SI-system (see Figure 10). The latter ones are described by the function

$$\lambda(x) = ax^2 + bx + c = -1.079(15) \cdot 10^{-7}x^2 - 0.009510(3)x + 656.908(1) \quad (5)$$

with the measured wavelength as argument. We determined the two lines in the red range together with the FWHM of the peaks as their errors. Furthermore we calculated the corresponding wavelengths using the calibration  $\lambda(x)$  with the final error

$$\Delta\lambda(x) = \sqrt{(\Delta a \cdot x^2)^2 + (\Delta b \cdot x)^2 + (\Delta c)^2 + (\Delta x \cdot 2ax + \Delta x \cdot b)^2} \quad (6)$$

Our results are  $\lambda_{Cd} = 643.846(36)\text{nm}$  and  $\lambda_{\alpha} = 652.210(32)\text{nm}$  respectively. Compared to the value  $\lambda_{Cd,lit} = 643.847\text{nm}$  from [2] our measurement confirms the bibliographical reference. Within the obtained error estimate from the gaussian fit for  $\lambda_{\alpha}$  there are the possibilities for the spectral line to be from Th I ( $\lambda_{ThI} = 652.2044\text{nm}$ ) or N II ( $\lambda_{NII} = 652.233\text{nm}$ ). We assume this line to emerge from materials in the electrodes of the lamp.

## Conclusions

In this experiment we considered the normal Zeeman Effect of cadmium. Therefore, we utilized a Lummer-Gehrcke spectrometer and observed the emerging interference lines with an adjustable telescope. Measuring the distances between these lines we could determine Bohr's magneton to  $\mu_B = 8.6(7) \cdot 10^{-24} \frac{\text{J}}{\text{T}}$ . One finds the value from literature  $\mu_{B,lit} = 9.274 \cdot 10^{-24} \frac{\text{J}}{\text{T}}$  to lie within the range of the measuring error.

Furthermore the specific electron charge has been determined from  $\mu_B$  and we obtained  $e = 1.48(12) \cdot 10^{-19}\text{C}$  which coincides with the bibliographical reference of  $e = 1.60 \cdot 10^{-19}\text{C}$ .

The second part of the experiment consisted of the calibration of a CCD spectrometer followed by the measurement of two lines in the red range emerging from a Hg-Cd lamp. For the calibration a neon lamp has been used. Determining the errors of the occurring peaks by gaussian fits we finally achieved a transformation function for the calibration.

As a result we can state that the line  $\lambda_{Cd} = 643.846(36)\text{nm}$  corresponds to Cd. The comparison with the bibliographical reference yields a coincidence within the range of error.

# Tables of measurends and derived quantities

	our measurement			used hysteresis	
voltage [V]	increasing	decreasing		increasing	decreasing
0	0.004	0.004		0.004	0.004
1	0.075	0.066		0.075	0.066
2	0.155	0.13		0.155	0.13
3	0.223	0.199		0.223	0.199
4	0.291	0.252		0.291	0.252
5	0.362	0.326		0.362	0.326
6	0.425	0.39		0.425	0.39
7	0.495	0.446		0.495	0.446
8	0.557	0.507		0.557	0.507
9	0.637	0.571		0.637	0.571
10	0.688	0.624		0.688	0.624
11	0.723	0.682		0.723	0.682
12	0.766	0.745		0.766	0.745
13	0.807	0.786		0.807	0.786
14	0.867	0.826		0.867	0.826
15	0.87	0.866		0.87	0.866
16	0.885	0.885		0.885	0.885

Table I: Data for the hysteresis (see Figure 2).

considered lines	2,3	3,4	4,5	5,6	6,7	7,8	8,9	9,10	10,11	11,12	12,13	13,14	14,15	15,16
$\Delta a$ [mm]	0,26	0,21	0,17	0,17	0,14	0,13	0,13	0,12	0,1	0,11	0,1	0,1	0,1	0,09

Table II: The considered lines correspond to the orders of the  $\pi$ -lines of the interference pattern.  $\Delta a$  denotes the distance between the according lines.

line	$\delta a$ [mm] $B = 0.688\text{T}, \sigma^-$	$\delta a$ [mm] $B = 0.688\text{T}, \sigma^+$	$\delta a$ [mm] $B = 0.766\text{T}, \sigma^-$	$\delta a$ [mm] $B = 0.766\text{T}, \sigma^+$	$\delta a$ [mm] $B = 0.867\text{T}, \sigma^-$	$\delta a$ [mm] $B = 0.867\text{T}, \sigma^+$	$\delta a$ [mm] $B = 0.885\text{T}, \sigma^-$	$\delta a$ [mm] $B = 0.885\text{T}, \sigma^+$
2	0.08	0.08	0.1	0.1	0.1	0.1	0.11	0.12
3	0.07	0.07	0.08	0.08	0.11	0.07	0.12	0.09
4	0.07	0.05	0.07	0.06	0.08	0.06	0.08	0.07
5	0.05	0.06	0.05	0.07	0.06	0.05	0.06	0.07
6	0.05	0.04	0.06	0.05	0.07	0.05	0.06	0.06
7	0.04	0.04	0.05	0.04	0.06	0.04	0.05	0.06
8	0.04	0.04	0.04	0.05	0.05	0.05	0.04	0.06
9	0.04	0.04	0.04	0.04	0.05	0.04	0.04	0.06
10	0.04	0.04	0.04	0.03	0.05	0.03	0.03	0.06
11	0.02	0.05	0.02	0.03	0.03	0.05	0.01	0.06
12	0.03	0.03	0.02	0.03	0.04	0.04	0.03	0.06
13	0.02	0.04	0.03	0.04	0.04	0.04	0.02	0.05
14	0.02	0.04	0.03	0.04	0.04	0.04	0.04	0.05
15	0.02	0.03	0.03	0.03	0.05	0.03	0.03	0.05
16	0.03	0.03	0.03	0.03	0.05	0.02	0.03	0.05

line	$\Delta\lambda$ [nm] $B = 0.688\text{T}, \sigma^-$	$\Delta\lambda$ [nm] $B = 0.688\text{T}, \sigma^+$	$\Delta\lambda$ [nm] $B = 0.766\text{T}, \sigma^-$	$\Delta\lambda$ [nm] $B = 0.766\text{T}, \sigma^+$	$\Delta\lambda$ [nm] $B = 0.867\text{T}, \sigma^-$	$\Delta\lambda$ [nm] $B = 0.867\text{T}, \sigma^+$	$\Delta\lambda$ [nm] $B = 0.885\text{T}, \sigma^-$	$\Delta\lambda$ [nm] $B = 0.885\text{T}, \sigma^+$
2	0.0149	0.0149	0.0186	0.0186	0.0186	0.0186	0.0204	0.0223
3	0.0161	0.0161	0.0184	0.0184	0.0253	0.0161	0.0276	0.0207
4	0.0199	0.0142	0.0199	0.0170	0.0227	0.0170	0.0227	0.0199
5	0.0142	0.0170	0.0142	0.0199	0.0170	0.0142	0.0170	0.0199
6	0.0173	0.0138	0.0207	0.0172	0.0242	0.0172	0.0207	0.0207
7	0.0149	0.0149	0.0186	0.0149	0.0223	0.0149	0.0186	0.0223
8	0.0149	0.0149	0.0149	0.0186	0.0186	0.0186	0.0149	0.0223
9	0.0161	0.0161	0.0161	0.0161	0.0201	0.0161	0.0161	0.0242
10	0.0194	0.0193	0.0193	0.0145	0.0242	0.0145	0.0145	0.0290
11	0.0088	0.0220	0.0088	0.0132	0.0132	0.0220	0.0044	0.0264
12	0.0145	0.0145	0.0096	0.0145	0.0193	0.0193	0.0145	0.0290
13	0.0097	0.0193	0.0145	0.0193	0.0193	0.0193	0.0096	0.0242
14	0.0096	0.0193	0.0145	0.0193	0.0193	0.0193	0.0193	0.0242
15	0.0107	0.0161	0.0161	0.0161	0.0269	0.0161	0.0161	0.0269

Table IV: The lines in the first column denote the orders of the interference pattern detected by the telescope.

$B$ [T]	$\overline{\Delta\lambda}$ [nm]	$\Delta(\overline{\Delta\lambda})$ [nm]	$\mu_B$ [J/T]	$\Delta\mu_B$ [J/T]
0.688	0.0155	0.0023	7.43E-24	1.12E-24
0.766	0.0165	0.0023	7.93E-24	1.13E-24
0.868	0.0191	0.0026	9.17E-24	1.24E-24
0.885	0.0203	0.0042	9.75E-24	2.01E-24

Table V:  $\overline{\Delta\lambda}$  denotes the mean value of  $\Delta\lambda$ .

	line position [px]	FWHM [px]	NIST-references [nm]	
neon	1915.2	4.1	638.29914	
neon	1720.8	4.0	640.2248	
neon	652.94	2.96	650.65277	
neon	379.04	3.10	653.28824	
	measured position [px]	FWHM [px]	calculated wavelength [nm]	error [nm]
	1352.8	3.6	643.8459	0.0356
	491.24	3.31	652.2104	0.0318

Table VI: Data for the calibration and determined wavelengths.

## References

- [1] Leybold Physics Leaflets, P6.2.7.1
- [2] <http://www.nist.gov>